



MEG3 LncRNA from Exosomes Released from Cancer-Associated Fibroblasts Enhances Cisplatin Chemoresistance in SCLC via a MiR-15a-5p/CCNE1 Axis

Yulu Sun^{1*}, Guijun Hao^{1*}, Mengqi Zhuang¹, Huijuan Lv², Chunhong Liu¹, and Keli Su¹

¹Department of Oncology, The Fourth People's Hospital of Jinan, Jinan;

²Department of Oncology, The Third Affiliated Hospital of Shandong First Medical University, Jinan, China.

Purpose: Long non-coding RNAs (lncRNAs) may act as oncogenes in small-cell lung cancer (SCLC). Exosomes containing lncRNAs released from cancer-associated fibroblasts (CAF) accelerate tumorigenesis and confer chemoresistance. This study aimed to explore the action mechanism of the CAF-derived lncRNA maternally expressed gene 3 (MEG3) on cisplatin (DDP) chemoresistance and cell processes in SCLC.

Materials and Methods: Quantitative real-time PCR was conducted to determine the expression levels of MEG3, miR-15a-5p, and CCNE1. Cell viability and metastasis were measured by 3-(4, 5-dimethyl-2-thiazolyl)-2, 5-diphenyl-2-h-tetrazolium bromide and invasion assays, respectively. A xenograft tumor model was developed to confirm the effect of MEG3 overexpression on SCLC progression in vivo. Relationships between miR-15a-5p and MEG3/CCNE1 were predicted using StarBase software and validated by dual luciferase reporter assay. Western blotting was used to determine protein levels. A co-culture model was established to explore the effects of exosomes on MEG3 expression in SCLC cell lines.

Results: MEG3 was overexpressed in SCLC tissues and cells. MEG3 silencing significantly repressed cell viability and metastasis in SCLC. High expression of MEG3 was observed in CAF-derived conditioned medium (CM) and exosomes, and promoted chemoresistance and cancer progression. Additionally, MEG3 was found to serve as a sponge of miR-15a-5p to mediate CCNE1 expression. Overexpression of miR-15a-5p and knockout of CCNE1 reversed the effects of MEG3 overexpression on cell viability and metastasis.

Conclusion: MEG3 lncRNA released from CAF-derived exosomes promotes DDP chemoresistance via regulation of a miR-15a-5p/CCNE1 axis. These findings may provide insight into SCLC therapy.

Key Words: Small-cell lung cancer, cancer-associated fibroblasts, exosomes, MEG3, chemoresistance

INTRODUCTION

Lung cancer is a highly invasive, rapidly metastasizing cancer

Received: September 1, 2021 **Revised:** November 5, 2021

Accepted: November 16, 2021

Corresponding author: Keli Su, MD, Department of Oncology, The Fourth People's Hospital of Jinan, No.50, Shifan Road, Jinan, Shandong 250031, China.
Tel: 86-15665172775, Fax: 86-0531-81313106, E-mail: jnslsy20203106@163.com

*Yulu Sun and Guijun Hao contributed equally to this work.

•The authors have no potential conflicts of interest to disclose.

© Copyright: Yonsei University College of Medicine 2022

This is an Open Access article distributed under the terms of the Creative Commons Attribution Non-Commercial License (<https://creativecommons.org/licenses/by-nc/4.0>) which permits unrestricted non-commercial use, distribution, and reproduction in any medium, provided the original work is properly cited.

with extremely low 5-year survival rates. Depending on histotype, prognosis, and treatment, lung cancer is generally divided in non-small cell lung cancer (NSCLC) and small-cell lung cancer (SCLC).¹ Compared to NSCLC, SCLC is more aggressive due to rapid growth and early metastasis.² The standard therapies for SCLC have not changed over the past three decades. A combination of etoposide/topotecan plus cisplatin (DDP) is the first-line therapy for SCLC.³ Although cases of SCLC are decreasing each year, SCLC still exhibits a low 5-year survival rate of less than 5%.⁴ Therefore, exploring hidden molecular mechanisms of SCLC and potential treatment targets are urgently needed for SCLC.

Increasing attention has paid to the tumor microenviron-

ment formed by interactions between tumor and stroma cells, which are closely correlated with immune evasion and cancer metastasis.⁵ Cancer-associated fibroblasts (CAF) are the main component of the tumor microenvironment and generally play a promoting role in tumor progression through the secretion of exosomes, an extracellular membranous vesicle containing DNA and various forms of RNA that acts as a vehicle in support of cell-to-cell communication.⁶ Numerous studies have reported that CAF-derived exosomal long non-coding RNAs (lncRNAs) are deeply involved in cancer progression and immune evasion.⁷⁻¹⁰ For instance, colorectal cancer-associated lncRNA or H19 has been found to facilitate chemoresistance in colorectal cancer.^{7,8} Exosomes lncRNA LINC00355 secreted from CAFs of bladder cancer have been shown to accelerate cell proliferation and metastasis, eventually aggravating the malignant behaviors of bladder cancer. Similarly, in esophageal squamous cell carcinoma, the exosomal lncRNA POU class 3 homeobox 3 (POU3F3) released from tumor cells has been found to promote DDP chemoresistance via activation of CAFs.¹⁰ In terms of lncRNA MEG3, Zhang, et al.¹¹ observed high expression of MEG3 in cervical cancer cell-secreted exosomes. In addition, Narayanan, et al.¹² analyzed differently expressed lncRNAs in tumor tissues of SCLC patients and found that MEG3 is overexpressed in SCLC patients. However, definitive research on whether CAF-derived lncRNA MEG3 is associated with SCLC DDP chemoresistance and progression is lacking.

In recent years, increasing evidence has indicated the anti-tumor roles of microRNAs (miRNAs) in SCLC.¹³⁻¹⁵ Wu, et al.¹³ demonstrated that significant reductions in proliferation and metastasis were observed in SCLC cells after transfection of miR-579-3p mimics. Zeng, et al.¹⁴ revealed that miR-218 is a downstream target of lncRNA LINC00173 and that high expression of miR-218 confers better prognosis among SCLC patients. Ye, et al.¹⁵ reported that overexpressed miR-495 represses chemoresistance and cell proliferation by mediating TSPAN12 expression in SCLC. Interestingly, miR-15a-5p has been identified as an anti-tumor miRNA in neuroblastoma,¹⁶ endometrial cancer,¹⁷ and breast cancer.¹⁸ Furthermore, overexpression of miR-15a-5p was also found to suppress lung cancer metastasis through regulation of histone acetylation,¹⁹ and miR-15a-5p could target CNKSR3 to affect NSCLC progression.²⁰ However, the possible role of miR-15a-5p in SCLC tumorigenesis and whether MEG3 regulates miR-15a-5p in SCLC remain unclear.

Cyclin E1 (CCNE1), an oncogene in several types of human cancer, has a positive effect on tumorigenesis.²¹⁻²⁴ Up-regulation of CCNE1 is observed in various human malignancies and is associated with poor prognosis.²⁴ Notably, a study conducted by Walter, et al.²⁵ demonstrated that overexpression of CCNE1 remarkably expedites cell cycle progression in SCLC. However, there are few studies on the interaction of CCNE1 with MEG3/miR-15a-5p in SCLC progression.

In the current study, the influences of MEG3 on DDP chemoresistance were investigated. We also determined whether MEG3 can be transferred from CAFs to cancer cells via exosomes, eventually affecting the progression of SCLC. In addition, potential regulatory mechanisms of a MEG3/miR-15a-5p/CCNE1 axis on SCLC tumorigenesis were explored. Our findings, for the first time, revealed that MEG3 from CAF-derived exosomes may contribute to DDP chemoresistance in SCLC through regulation of a miR-15a-5p/CCNE1 axis.

MATERIALS AND METHODS

SCLC samples and isolation of primary fibroblasts

The study was approved by the Institutional Review Board of The Fourth People's Hospital of Jinan (approval ID: 2017-12-17), and written informed consent was provided by all study patients. A total of 48 patients diagnosed with primary SCLC from December 2018 to January 2020 was recruited in our hospital. None of the volunteers had received any treatments before admission. Tumor tissues and corresponding normal tissues (5 cm from the outer tumor margin) were subjected to histological examination and then collected for determining the expression of MEG3, miR-15a-5p, and CCNE1. Afterwards, the aforementioned tissues were immediately washed with sterile PBS, followed by digestion with collagenase type I to isolate primary CAFs and normal fibroblasts (NF), respectively. CAFs and NFs were further identified by the presence of CAF-specific markers (FAP, FSP1, and α -SMA) by Western blot assay. For the preparation of CAF-conditioned medium (CAF-CM) and NF-CM, isolated CAFs and NFs were cultured in Dulbecco's Modified Eagle's Medium (DMEM)/F12 supplemented with 10% fetal bovine serum (FBS) at 37°C, 5% CO₂ for 48 h, and then collected and centrifuged to remove cell debris. All fibroblasts used in this study were subjected to fewer than 10 passages.

Cell culture

SCLC cell lines (NCI-H69 and NCI-H446) and the normal bronchial epithelial cell line 16HBE were procured from the American Type Culture Collection (Manassas, VA, USA) and grown in DMEM containing 10% FBS in an incubator with 5% CO₂ at 37°C.

Quantitative real-time PCR

Total RNA was extracted from tissues, cell lines, and CAFs using Total RNA Extraction Kits (Solarbio Science & Technology, Beijing, China) and synthesized to cDNA using the First-Strand cDNA Synthesis Kit (APEX BIO Technology, Houston, TX, USA), followed by performing qRT-PCR with SYBR Green FAST Mastermix (Qiagen, Dusseldorf, Germany). The 2^{- $\Delta\Delta$ CT} method was utilized to calculate relative expression. GAPDH and U6 were used as internal controls.

Cell transfection

Small hairpin RNA targeting MEG3 (sh-MEG3), sh-CCNE1, and the corresponding negative control (sh-NC), vector over-expressing MEG3 (pcDNA3.1-MEG3), empty vector (pcDNA3.1-NC), miR-15a-5p inhibitor/inhibitor negative control, and miR-15a-5p mimics/mimics negative control were all purchased from VectorBuilder (Guangzhou, China). The transfection experiments were performed using Lipofectamine 3000 (Invitrogen, Nanjing, China) according to provided instructions. After transfection for 48 h, cells were collected for subsequent experiments.

3-(4, 5-dimethyl-2-thiazolyl)-2, 5-diphenyl-2-h-tetrazolium bromide (MTT) assay

The viability of SCLC cells was detected by MTT assay. The transfected SCLC cell lines were seeded into a 96-well plate at 2×10^5 cells per well. Subsequently, the cells were incubated for 24, 48, 72, and 96 h, followed by adding 20 μ L of MTT (GENECHEM, Inc, Shanghai, China) to each well for incubation 2 h at 37°C. For the measurement of DDP chemoresistance in SCLC cells, increasing doses of DDP (0, 0.625, 1.25, 2.5, 5, 10, 20, and 40 μ M) were used to treat the transfected SCLC cells. Viability (OD450) was determined using a microplate reader (Thermo Fisher Scientific, Waltham, MA, USA).

Transwell assay

For migration assay, the transfected NCI-H69 and NCI-H446 cells (5×10^4) were re-suspended in serum-free DMEM and seeded into the upper chamber. At the same time, the lower chamber was treated with DMEM containing 10% FBS. For the invasion assay, Matrigel procured from BD Company was used to coat the membranes before adding the cells. Following incubation overnight at 37°C, cells in the lower chamber were stained with 0.1% crystal violet for 15 min. A light microscope (magnification, $\times 400$) was used to count stained cells in five randomly-selected fields.

SCLC mouse model

BALB/c nude mice weighing 22–24 g (4–5 week; EseBio, Shanghai, China) were assigned into the pcDNA3.1-MEG3 group and pcDNA3.1-NC group (n=5) *ad libitum*. Then, pcDNA3.1-MEG3 or pcDNA3.1-NC was transfected into NCI-H69 cells. We then anesthetized the mice using pentobarbital sodium (50 mg/kg) and subcutaneously injected the transfected NCI-H446 cells (1×10^6). Approximately 6 weeks later, all mice were sacrificed, and the solid tumors were collected. Tumor volume was calculated with the formula $V = 1/2 [(tumor\ length) \times (tumor\ width)]^2$.

Isolation of exosomes

CAFs and NFs were cultured in DMEM/F12 containing 10% FBS without exosomes at 37°C with 5% CO₂. After 48 h of culture, the supernatant and cell fragments were separated by

centrifugation. Exosomes were isolated from the collected supernatant using a GM Exosome Isolation Reagent kit (GeneSeed Biology, Inc, Guangzhou, China), followed by incubation at 4°C for 30 min. The isolated exosomes were resuspended in PBS. The exosomes were observed under a transmission electron microscopy and determined using the surface markers of exosomes CD63 (positive marker), HSP70 (positive marker), and GM130 (negative marker) by Western blotting.

Fluorescence-labeled exosomes and uptake of the exosomes

Based on the manufacturer's instructions, the Exo-Green fluorescent staining kit PKH67 (Yanzai Biology, Ltd, Shanghai, China) was used to label the exosomes. In brief, the exosomes were re-suspended with PBS, mixed with Exo-Green, and incubated for 10 min. After the mixture was centrifuged, the precipitates (containing exosomes) were re-suspended with PBS. Cells (1×10^5) were seeded into a 35-mm dish. Subsequently, the labeled exosomes (100 μ L) were added, cultured for 24 h, and observed under a confocal microscope (scale bar=100 μ m).

Western blot assay

The isolated CAFs, exosomes, and protein levels of CCNE1 were determined by Western blotting. The procedures were performed as follows: the extracted proteins were initially lysed with RIPA buffer, followed by determination of protein concentrations using a BCA Protein Assay Kit (Thermo Fisher Scientific). Afterwards, the proteins were separated by 10% SDS-PAGE and then transferred into PVDF membranes, in which incubation with relevant primary antibodies (1:1000) at 4°C overnight and with secondary antibody (1:5000) for 1 h at room temperature. GAPDH was used as the internal control. Immunoblots were visualized using an ECL detection kit (Amersham Biosciences, Uppsala, Sweden).

Dual-luciferase reporter assay

The binding sites between miR-15a-5p and MEG3/CCNE1 were predicted using StarBase software (<http://starbase.sysu.edu.cn/index.php>). For dual-luciferase reporter assay, the fragments of MEG3 or CCNE1 containing miR-15a-5p binding sites, including wild type (wt) and mutant type (mut), were initially inserted into pGL3 vector to establish the recombinant reporter plasmids. Subsequently, NCI-H446 cells (4000 cells/well) were co-transfected with miR-15a-5p mimics/mimics NC, and MEG3/CCNE1 wt or mut using Lipofectamine 3000 (Invitrogen, Carlsbad, CA, USA) and incubated at 48 h 37°C. A dual-luciferase reporter assay system (Promega, Madison, WI, USA) was used to detect the luciferase activity.

Statistical analysis

Data are presented as means \pm SD and were analyzed using SPSS 20.0 software (IBM Corp., Armonk, NY, USA). Student's t-test was utilized for comparisons between two groups. One-

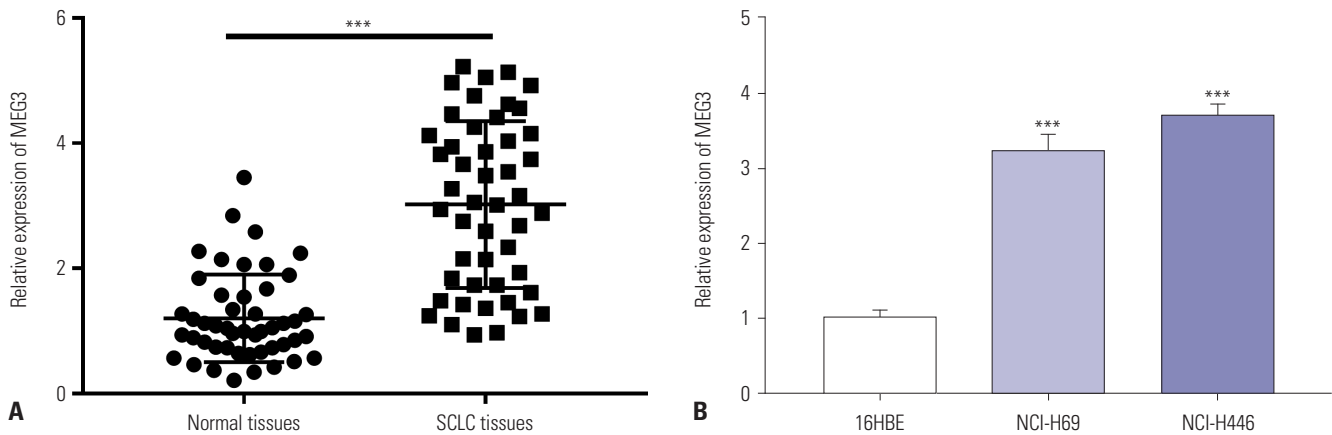


Fig. 1. High expression of MEG3 in SCLC tissues and cell lines. (A) The expression of MEG3 in SCLC tissues (n=48) and normal tissues (n=48) was detected by qRT-PCR. ****p*<0.001 vs. the normal tissues. (B) The expression of MEG3 in SCLC cells (NCI-H69 and NCI-H446) and normal bronchial epithelial cells (16HBE) was detected by qRT-PCR. ****p*<0.001 vs.16HBE cells. SCLC, small-cell lung cancer.

way ANOVA was used to evaluate differences among multiple groups, followed by Tukey’s multiple comparisons test. *p* values less than 0.05 indicated a statistically significant difference.

RESULTS

High expression of MEG3 in SCLC tissues and cell lines associated with clinical stage

The expression of MEG3 in SCLC tissues was detected. We found that compared to the normal tissues, relatively higher expression of MEG3 was exhibited in SCLC tissues (*p*<0.001) (Fig. 1A). We then assessed MEG3 expression in SCLC cell lines. The results of qRT-PCR demonstrated that MEG3 was upregulated in NCI-H69 and NCI-H446 cells, compared with that in 16HBE cells (*p*<0.001) (Fig. 1B). In addition, we also determined the correlation between the expression of MEG3 and clinicopathological characteristics in SCLC. As shown in Table 1, high expression of MEG3 was strongly correlated with clinical stage in SCLC (*p*=0.008).

Silencing of MEG3 inhibits cell viability and metastasis in SCLC

Afterwards, pcDNA3.1-MEG3/NC or sh-MEG3/NC was transfected into both NCI-H69 and NCI-H446 cells to determine the transfection efficiency. As presented in Fig. 2A, the expression of MEG3 was increased by transfection with pcDNA3.1-MEG3, but decreased by sh-MEG3 (*p*<0.001). NCI-H69 and NCI-H446 cells transfected with sh-MEG3 were used for the following functional experiments on account of the high expression of MEG3 observed in clinical pathologic tissues and SCLC cell lines. As illustrated in Fig. 2B-D, silencing of MEG3 significantly restrained cell viability, migration, and invasion in SCLC (*p*<0.05).

Table 1. Correlations between MEG3 Expression and Clinicopathological Characteristics in SCLC

Characteristics	Total	MEG3 expression		<i>p</i> value
		Low (n=24)	High (n=24)	
Age				0.773
<55 years	22	10	12	
≥55 years	26	14	12	
Sex				0.372
Male	30	17	13	
Female	18	7	11	
Tumor size (cm)				0.380
<5	28	16	12	
≥5	20	8	12	
Smoking				0.227
No	17	11	6	
Yes	31	13	18	
Clinical stage				0.008*
Limited disease	26	18	8	
Extensive-stage disease	22	6	16	

SCLC, small-cell lung cancer.

**p*<0.05.

Overexpressed MEG3 enhances DDP chemoresistance in SCLC

To explore whether MEG3 affects chemoresistance to DDP, the cell viabilities of NCI-H69 and NCI-H446 cells transfected with pcDNA3.1-MEG3/NC were measured by MTT assay. We found that MEG3 overexpression resulted in DDP resistance in both NCI-H69 and NCI-H446 cells (*p*<0.05) (Fig. 3A). In addition, we also demonstrated that the overexpression of MEG3 significantly accelerated the growth of tumor xenografts in a mouse model (*p*<0.01) (Fig. 3B and C). At the same time, the expression of MEG3 in mice injected with pcDNA3.1-MEG3 was increased, compared to injection of pcDNA3.1-NC (*p*<0.01) (Fig. 3D).

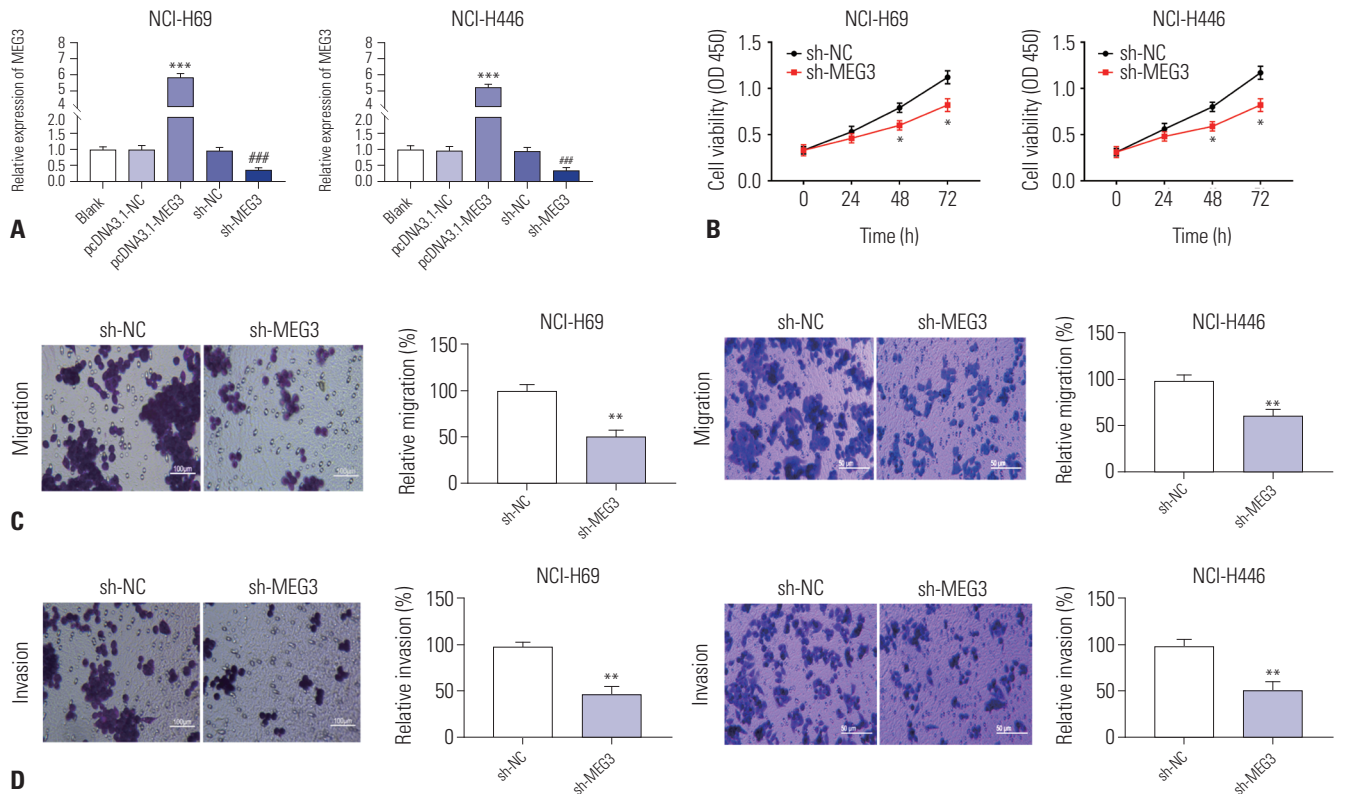


Fig. 2. MEG3 silencing inhibits cell viability and metastasis in SCLC. (A) The expression of MEG3 after transfection of sh-MEG3/NC or pcDNA3.1-MEG3/NC into SCLC cells (NCI-H69 and NCI-H446) was detected by qRT-PCR. *** $p < 0.001$ vs. the pcDNA3.1-NC group, ### $p < 0.001$ vs. the sh-NC group. (B) The viability of SCLC cells transfected with sh-MEG3/NC was measured by MTT assay. (C) The migration of SCLC cells transfected with sh-MEG3/NC was measured by transwell migration assay. (D) The invasion of SCLC cells transfected with sh-MEG3/NC was measured by transwell invasion assay. * $p < 0.05$, ** $p < 0.01$ vs. the sh-NC group. SCLC, small-cell lung cancer.

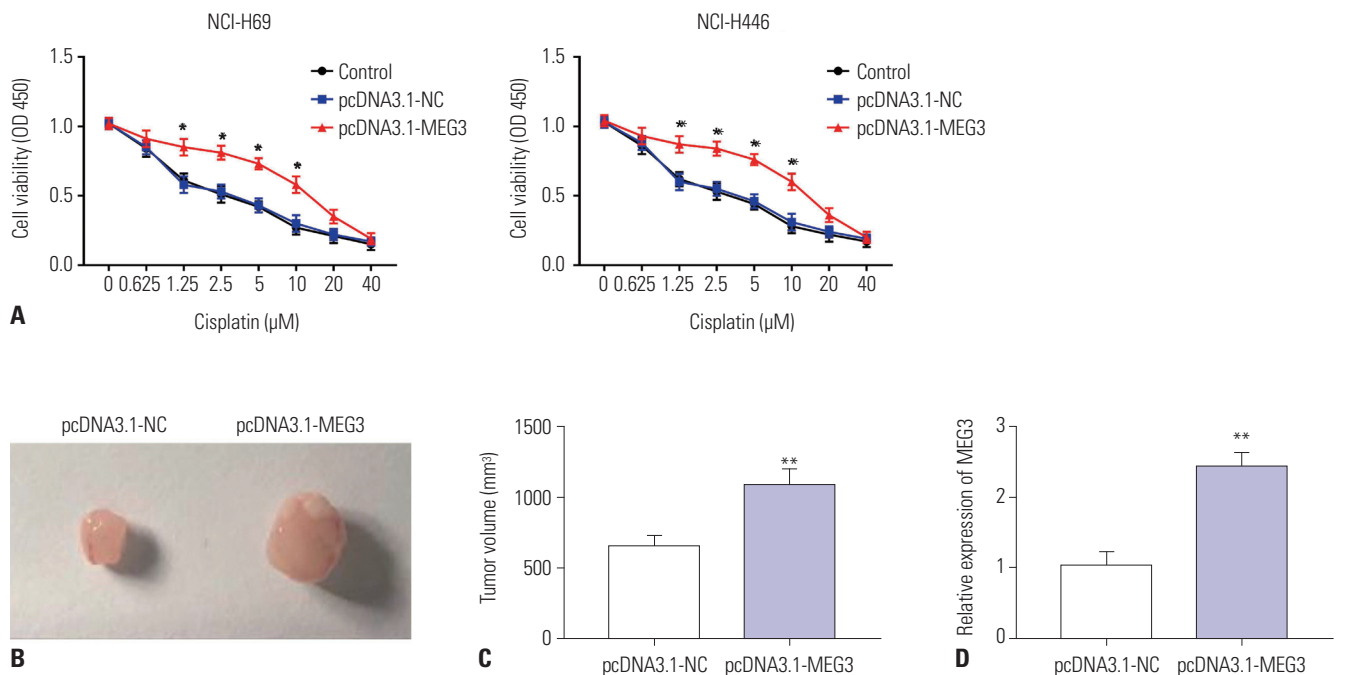


Fig. 3. Overexpression of MEG3 enhances DDP chemoresistance in SCLC. (A) The viability of SCLC cells transfected with pcDNA3.1-MEG3/NC under different concentrations of DDP (0, 0.625, 1.25, 2.5, 5, 10, 20, and 40 μM) was measured by MTT assay. (B) Image of a solid tumor after injection of pcDNA3.1-MEG3/NC. (C) Tumor volume after injection of pcDNA3.1-MEG3/NC. (D) The expression of MEG3 in tumor xenograft tissues injected with pcDNA3.1-MEG3/NC was detected by qRT-PCR. * $p < 0.05$, ** $p < 0.01$ vs. the pcDNA3.1-NC group. SCLC, small-cell lung cancer.

CAFs facilitate metastasis and DDP chemoresistance among SCLC cells

In order to explore the origin and role of MEG3 in SCLC, we isolated CAFs and NFs from SCLC tissues and adjacent normal tissues, respectively. The protein levels of CAF-specific markers were determined by Western blot assay. As shown in Fig. 4A, we discovered that the levels of FAP, FSP1, and α -SMA were significantly elevated in CAFs, compared to those in NFs ($p < 0.05$), suggesting that CAF was isolated successfully. As expected, the expression of MEG3 in CAFs was higher than that in NFs ($p < 0.001$) (Fig. 4B). We then assessed the effects of CAF-CM on cell metastasis and DDP chemoresistance. Transwell assay revealed that compared with NF-CM, CAF-CM markedly enhanced the migration and invasion of NCI-H69 and NCI-H446 cells ($p < 0.01$) (Fig. 4C and D). Afterwards, SCLC cells grown in CAF-CM and subsequently treated with DDP showed a significant increase in cell viability, compared with those grown in NF-CM ($p < 0.05$) (Fig. 4E).

Overexpression of MEG3 is found in CAF-derived exosomes

Numerous studies have reported that CAF-derived exosomes are strongly correlated with cancer progression.⁸⁻¹⁰ Therefore, the relationship between CAF-derived exosomes and MEG3 expression in SCLC was further investigated. An exosome inhibitor (GW4869) was used to suppress the secretion of exosomes, and then, MEG3 expression was detected in CAF-CM. We found that MEG3 expression could be induced by CAF-CM ($p < 0.001$) (Fig. 5A), but was inhibited by GW4869 treatment ($p < 0.01$). We then purified exosomes from CAFs and NFs. Under a transmission electron microscope, the isolated exosomes appeared as round membranous vesicles (30–60 nm) in accordance with the characteristics of exosomes (Fig. 5B). The exosomes were further validated by Western blot assay, and we found that the isolated exosomes expressed exosome-positive protein markers, including CD63 and HSP70, but not the negative marker GM130 ($p < 0.05$) (Fig. 5C). In addition, we measured the expression levels of MEG3 in the isolated exosomes and observed that MEG3 was overexpressed in the CAF-Exo

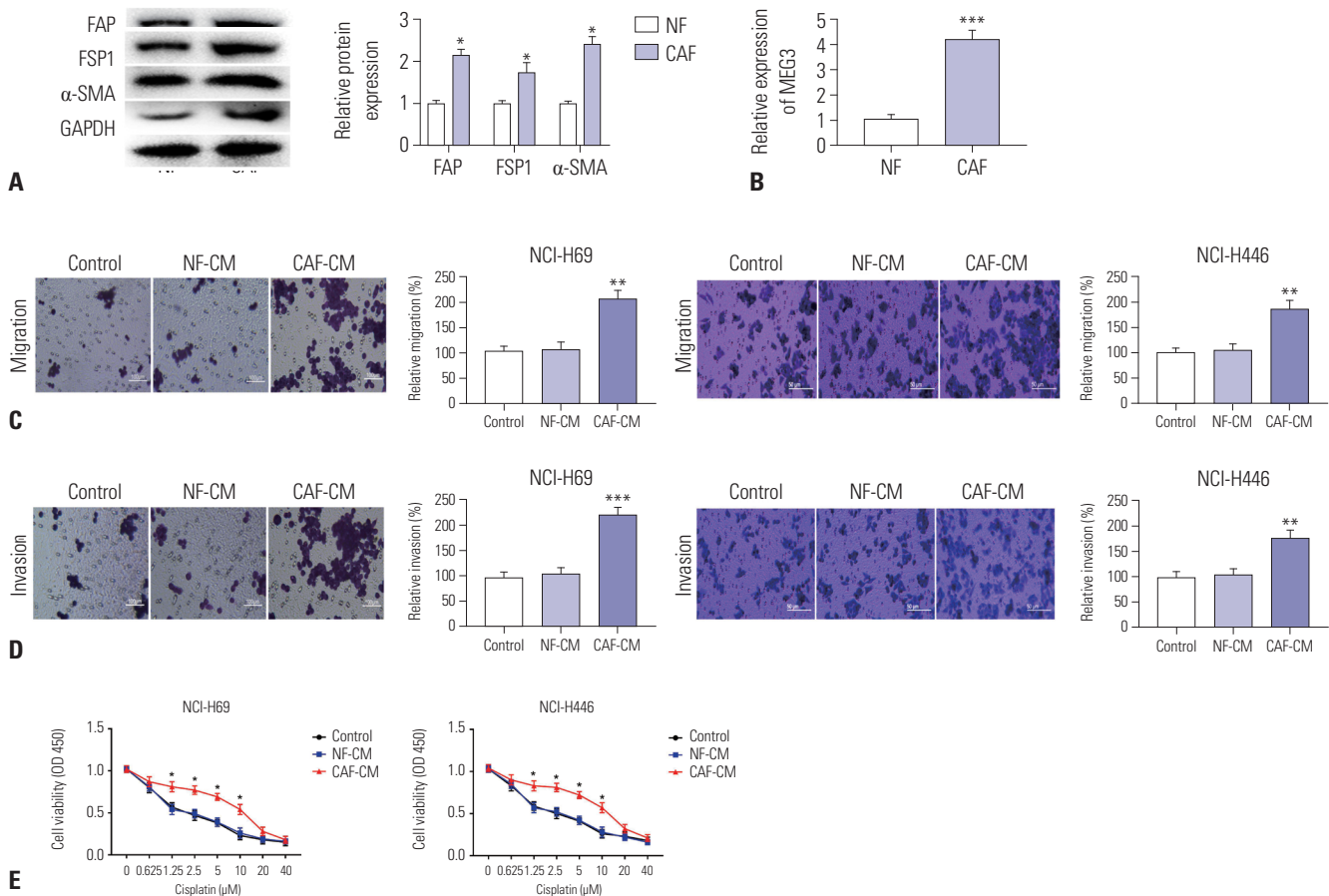


Fig. 4. CAF facilitates metastasis and DDP chemoresistance among SCLC cells. (A) The proteins levels of FAP, FSP1, and α -SMA in CAFs or NFs were determined by Western blot assay. * $p < 0.05$ vs. the NF group. (B) The expression of MEG3 in CAFs or NFs. *** $p < 0.001$ vs. the NF group. (C) The migration of SCLC cells grown in CAF-CM or NF-CM was measured by transwell migration assay. (D) The invasion of SCLC cells grown in CAF-CM or NF-CM was measured by transwell invasion assay. (E) The viability of SCLC cells grown in CAF-CM or NF-CM under different concentrations of DDP (0, 0.625, 1.25, 2.5, 5, 10, 20, and 40 μ M) was measured by MTT assay. * $p < 0.05$, ** $p < 0.01$, *** $p < 0.001$ vs. the NF-CM group. SCLC, small-cell lung cancer; NF, normal fibroblasts; CAF, cancer-associated fibroblasts; CM, conditioned medium.

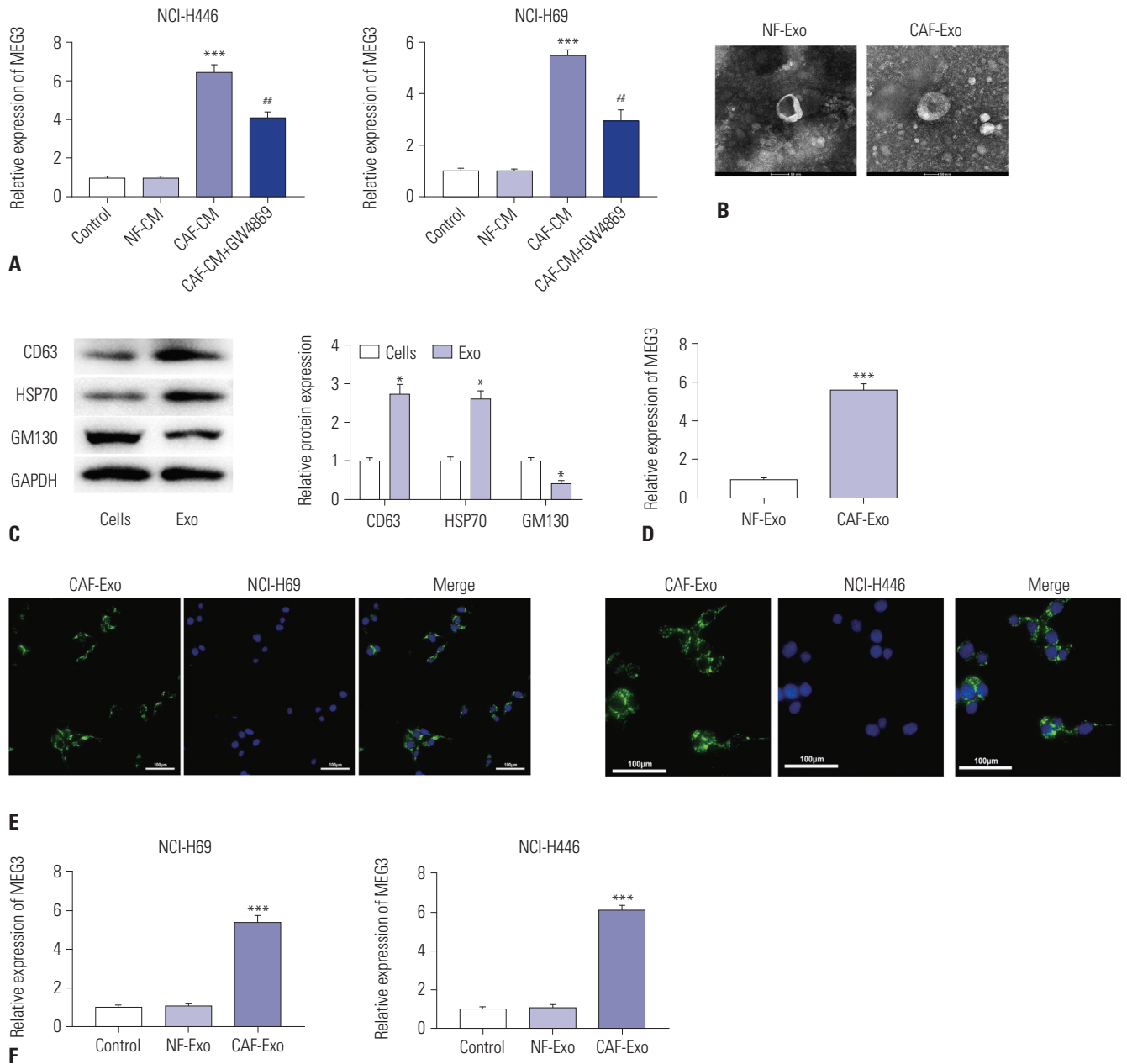


Fig. 5. Overexpression of MEG3 is found in CAF-derived exosomes. (A) The expression of MEG3 in SCLC cells under different CM was detected by qRT-PCR. *** $p < 0.001$ vs. the NF-CM group, ** $p < 0.01$ vs. the CAF-CM group. (B) The morphological characteristics of exosomes, which were round membranous vesicles, were observed by transmission electron microscopy. Scale bar: 50 nm. (C) The levels of exosomes surface markers (CD63, HSP70, and GM130) were detected by Western blot assay. * $p < 0.05$ vs. the whole cells group. (D) The expression of MEG3 in CAF-Exo or NF-Exo was detected by qRT-PCR. *** $p < 0.001$ vs. the NF-Exo group. (E) Uptake of CAF-derived exosomes was observed under a confocal microscope. (F) The expression of MEG3 in SCLC cells co-cultured with exosomes from CAFs or NFs was detected by qRT-PCR. *** $p < 0.001$ vs. the NF-Exo+SCLC cells (NCI-H69 and NCI-H446) group. SCLC, small-cell lung cancer; NF, normal fibroblasts; CAF, cancer-associated fibroblasts; CM, conditioned medium.

group, compared to NF-Exo ($p < 0.001$) (Fig. 5D). The fluorescence-labeled CAF-Exo was observed using a confocal microscope, and we found that CAF-derived exosomes were taken up by receptor cells (NCI-H69 and NCI-H446) and intensively distributed around the nucleus (Fig. 5E). Meanwhile, relatively high expression of MEG3 was also exhibited in both NCI-H69 and NCI-H446 cells co-cultured with exosomes from CAF ($p < 0.001$) (Fig. 5F).

Identification the miR-15a-5p/CCNE1 axis as a downstream target of MEG3 in SCLC

While the results above indicated that CAF-derived exosomes MEG3 may affect SCLC progression, detailed regulatory mechanisms thereof remained elusive. StarBase software was used to predict the binding site between MEG3 and miR-15a-5p, as well as between miR-15a-5p and CCNE1 (Fig. 6A). Dual-luciferase reporter assay demonstrated that transfection of miR-

15a-5p mimics could remarkably decrease the luciferase activity of MEG3 wt or CCNE1 wt reporter vector in NCI-H446 cells ($p < 0.01$) (Fig. 6B), suggesting that MEG3 targets miR-15a-5p and that miR-15a-5p further targets CCNE1. Thereafter, miR-15a-5p mimics/mimics NC or miR-15a-5p inhibitor/inhibitor NC was transfected into NCI-H446 cells to determine the trans-

fection efficiency. As illustrated in Fig. 6C, miR-15a-5p expression was increased by transfection with miR-15a-5p mimics and decreased by miR-15a-5p inhibitor ($p < 0.01$). We further found that miR-15a-5p expression could be upregulated by MEG3 knockdown ($p < 0.01$) (Fig. 6D), whereas CCNE1 protein levels were reduced by miR-15a-5p upregulation ($p < 0.01$) (Fig.

MEG3 wt: 5' cacacauguggccuUGCUGCUG 3'
 | | | | | | | |
miR-15a-5p : 3' guguuugguaauacACGACGAu 5'

MEG3 mut: 5' cacacauguggccuACGACGAg 3'

CCNE1 wt: 5' gugcgugcucccgaUGCUGCUa 3'
 | | | | | | | |
miR-15a-5p : 3' guguuugguaauacACGACGAu 5'

CCNE1 mut: 5' gugcgugcucccgaACGACGAa 3'

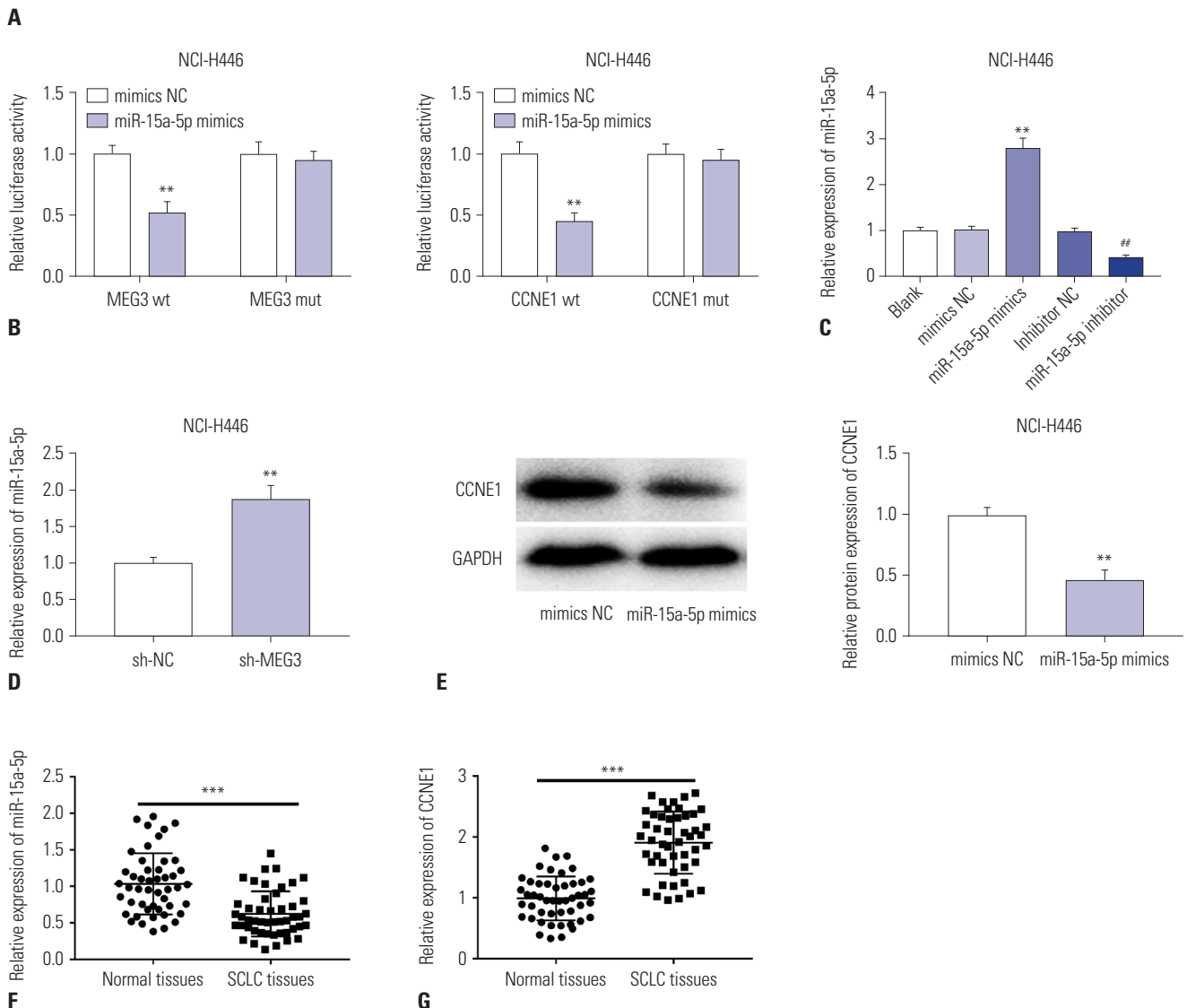


Fig. 6. Identification of a miR-15a-5p/CCNE1 axis as a downstream target of MEG3 in SCLC. (A) The predicted complementary binding sites between miR-15a-5p and MEG3/CCNE1. (B) The luciferase activity in NCI-H446 cells co-transfected with pGL3-MEG3 wt/pGL3-MEG3 mut and miR-15a-5p mimics/mimics NC or pGL3-CCNE1 wt/pGL3-CCNE1 mut and miR-15a-5p mimics/mimics NC was determined by dual luciferase reporter assay. $**p < 0.01$ vs. the mimics NC group. (C) The expression of miR-15a-5p after transfection of miR-15a-5p mimics/mimics NC or miR-15a-5p inhibitor/inhibitor NC into NCI-H446 cells was detected by qRT-PCR. $**p < 0.01$ vs. the mimics NC group, $\#p < 0.01$ vs. the inhibitor NC group. (D) The expression of miR-15a-5p in NCI-H446 cells transfected with sh-MEG3/NC was detected by qRT-PCR. $**p < 0.01$ vs. the sh-NC group. (E) The protein levels of CCNE1 in NCI-H446 cells transfected with miR-15a-5p mimics/mimics NC was determined by Western blot assay. $**p < 0.01$ vs. the mimics NC group. (F) The expression of miR-15a-5p in SCLC tissues ($n = 48$) and normal tissues ($n = 48$) was detected by qRT-PCR. $***p < 0.001$ vs. the normal tissues. (G) The expression of CCNE1 in SCLC tissues ($n = 48$) and normal tissues ($n = 48$) was detected by qRT-PCR. $***p < 0.001$ vs. the normal tissues. SCLC, small-cell lung cancer.

6E). Additionally, decreased miR-15a-5p or increased CCNE1 was observed in SCLC tissues, compared with the corresponding normal tissues ($p < 0.001$) (Fig. 6F and G).

Overexpressed MEG3 promotes DDP chemoresistance and metastasis in SCLC via a miR-15a-5p/CCNE1 axis

To explore the regulatory mechanisms among MEG3, miR-15a-5p, and CCNE1 on SCLC progression, feedback verifica-

tion experiments were performed in NCI-H446 cells. First, we detected the transfection efficiency of sh-CCNE1/NC. The results of qRT-PCR demonstrated that transfection of sh-CCNE1 significantly suppressed the expression of CCNE1 ($p < 0.01$) (Fig. 7A). Additionally, we showed that CCNE1 expression was elevated after transfection of pcDNA3.1-MEG3 ($p < 0.01$) (Fig. 7B); however, transfection of miR-15a-5p mimics reversed the promoting effect of MEG3 over-expression on CCNE1 levels

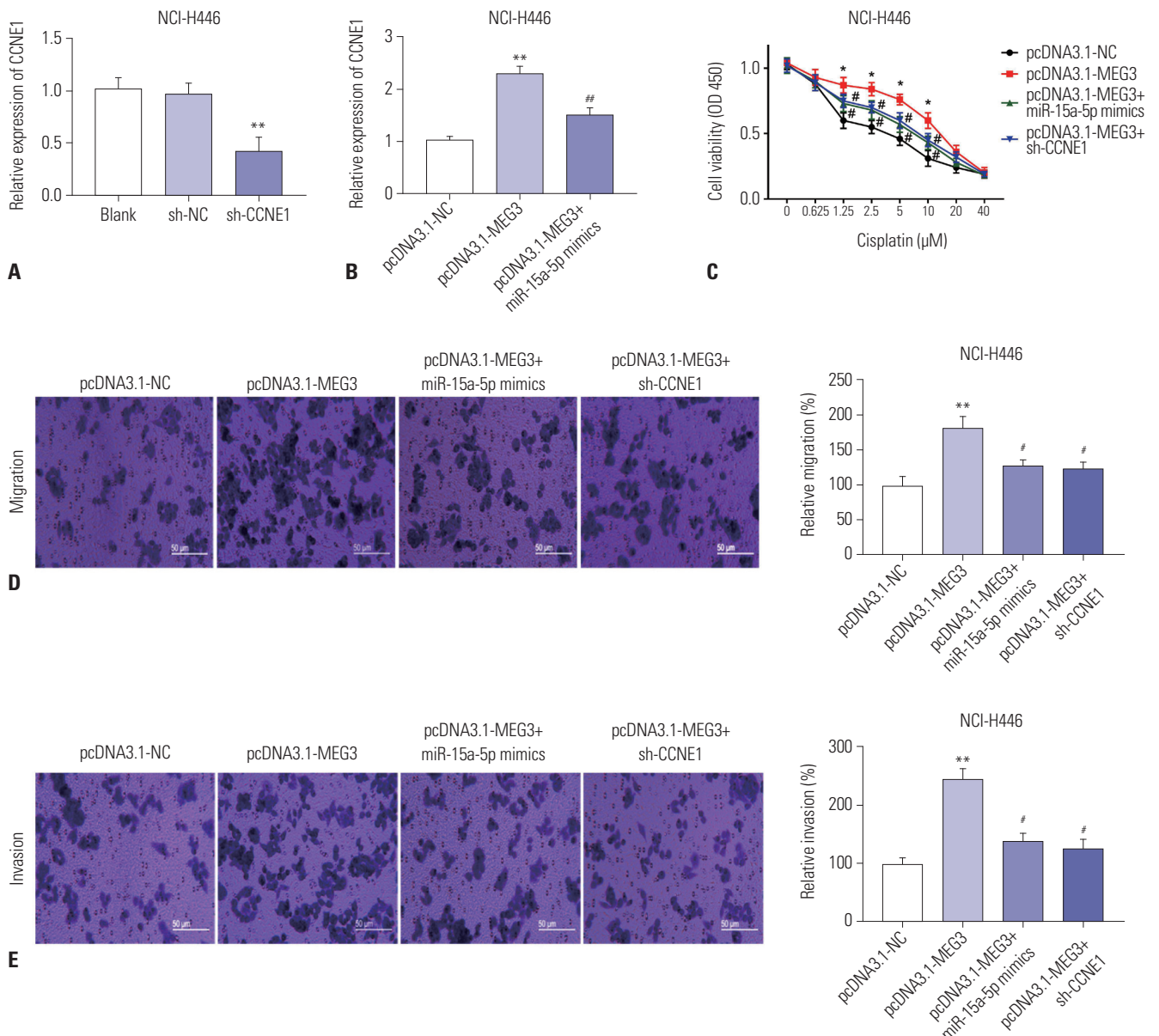


Fig. 7. Overexpression of MEG3 promotes DDP chemoresistance and metastasis in SCLC via the miR-15a-5p/CCNE1 axis. (A) The expression of CCNE1 in NCI-H446 cells after transfection with sh-CCNE1/NC was detected by qRT-PCR. ** $p < 0.01$ vs. the sh-NC group. (B) The expression of CCNE1 in NCI-H446 cells after transfection with pcDNA3.1-MEG3 or pcDNA3.1-MEG3+miR-15a-5p mimics was detected by qRT-PCR. ** $p < 0.01$ vs. the pcDNA3.1-NC group, # $p < 0.05$ vs. the pcDNA3.1-NC group. (C) The viability of NCI-H446 cells transfected with pcDNA3.1-NC, pcDNA3.1-MEG3, pcDNA3.1-MEG3+miR-15a-5p mimics, or pcDNA3.1-MEG3+sh-CCNE1 under different concentrations of DDP (0, 0.625, 1.25, 2.5, 5, 10, 20, and 40 μM) was measured by MTT assay. (D) The migration of NCI-H446 cells transfected with pcDNA3.1-NC, pcDNA3.1-MEG3, pcDNA3.1-MEG3+miR-15a-5p mimics, or pcDNA3.1-MEG3+sh-CCNE1 was measured by transwell migration assay. (E) The invasion of NCI-H446 cells transfected with pcDNA3.1-NC, pcDNA3.1-MEG3, pcDNA3.1-MEG3+miR-15a-5p mimics, or pcDNA3.1-MEG3+sh-CCNE1 was measured by transwell invasion assay. * $p < 0.05$, ** $p < 0.01$ vs. the pcDNA3.1-NC group, # $p < 0.05$ vs. the pcDNA3.1-MEG3 group. SCLC, small-cell lung cancer.

($p < 0.01$). Subsequently, feedback verification experiments were conducted. As presented in Fig. 7C-E, overexpressed MEG3 enhanced chemoresistance and cell metastasis in SCLC ($p < 0.05$). Both upregulation of miR-15a-5p and downregulation of CCNE1 reversed the promoting effects of MEG3 overexpression on the aforementioned cellular processes in SCLC ($p < 0.05$).

DISCUSSION

In recent decades, SCLC therapies have not greatly improved.¹⁴ DDP-based chemotherapy after surgical resection is still the most effective therapy for SCLC.^{26,27} Unfortunately, intrinsic or acquired resistance to DDP-based combinations affects the therapeutic effect to a large extent.⁷ Therefore, exploring underlying targets to enhance the susceptibility to DDP may be more helpful for SCLC treatment. Our results revealed that CAF transfers MEG3 via exosomes to interact with SCLC cells and eventually promotes DDP chemoresistance through regulation of a miR-15a-5p/CCNE1 axis.

The participation of lncRNAs in SCLC tumorigenesis has been confirmed in previous research.²⁸⁻³⁰ For example, Niu, et al.²⁹ discovered relatively high expression levels of taurine-up-regulated gene 1 (TUG1) in SCLC tissues and cells, which exhibited a strong correlation with clinical stage (limited stage and extensive stage). Sun, et al.³⁰ demonstrated that HOXA transcript at the distal tip (HOTTIP) expression in SCLC tissues and cells is upregulated and that the upregulation of HOTTIP is closely correlated to disease stage. Zhang, et al.²⁸ also revealed that overexpression of SBF2 antisense RNA 1 is correlated with SCLC stage. In the current study, we also found overexpression of MEG3 in SCLC tissues and cells. In line with our findings, Narayanan, et al.¹² also found that MEG3 is overexpressed in SCLC patients. Furthermore, high expression of MEG3 was also shown to have strong correlation with clinical stage in this study. Therefore, we speculated that MEG3 may act as an onco-lncRNA in SCLC.

Many lncRNAs act as promoters of carcinogenesis and chemoresistance in SCLC, whereas silencing of lncRNAs has inhibiting effects on SCLC progression.¹⁴ The lncRNA TUG1 for instance, knocked down by small interfering RNA sequences, not only repressed the growth of solid tumors, but also enhanced anticarcinogen chemosensitivity in SCLC.²⁹ Silencing of HOTTIP was found to accelerate apoptosis in SCLC and to eliminate resistance to cisplatin.³⁰ In contrast, overexpression of LINC00173 was confirmed to promote chemoresistance and cell metastasis in SCLC.¹⁴ Similarly, we found that MEG3 deletion inhibited proliferation and metastasis of SCLC cells *in vitro*. In addition, we further discovered that overexpression of MEG3 suppressed chemosensitivity to DDP among SCLC cells and facilitated the growth of tumor xenografts in a mouse model. Interestingly, we noticed that the overexpression of MEG3

exerts similar influences in several cancers, including lymphoma,³¹ breast cancer,³² and colorectal cancer.³³ Taking our findings together with previous results, we conjectured that MEG3 knockdown serves as a suppressor of SCLC. On the contrary, overexpression of MEG3 promotes DDP chemoresistance and tumor growth. Meanwhile, research has shown that lncRNAs generally exert their biological function by acting as miRNA sponges to modulate gene expression.³⁴ In this study, miR-15a-5p, which targets CCNE1, was determined as a target of MEG3. Interestingly, similar to previous studies, we observed downregulation of miR-15a-5p and upregulation of CCNE1 in SCLC tissues.^{25,35} Additionally, downregulation of miR-15a-5p reversed elevated levels of CCNE1 caused by MEG3 overexpression. Based on the above findings, we speculate that MEG3 may regulate DDP chemoresistance and tumor growth via sponging of miR-15a-5p via CCNE1. As expected, rescue experiments demonstrated that high expression of miR-15a-5p or low expression of CCNE1 reversed the promoting effects of MEG3 overexpression on chemoresistance and cell metastasis in SCLC, which validated our assumption.

Additionally, we explored the possible action mechanism of MEG3 on DDP chemoresistance and SCLC progression. Recently, numerous studies have reported that CAFs, the main component of the tumor microenvironment, play a key role in cancer cell metastasis³⁶ and drug resistance.³⁷ Therefore, CAFs and NFs were isolated successfully from SCLC patients in this study. We discovered that the metastasis capacities of SCLC cell lines grown in CAF-CM were significantly enhanced. At the same time, cancer cells cultured in CAF-CM also exhibited DDP chemoresistance. All of these findings were in line with previous studies.³⁸ Given that the above conclusion that MEG3 dysregulation is strongly associated with DDP chemoresistance and tumor growth, we further speculated that there may be some kind of connection between MEG3 and CAF. As expected, increased MEG3 expression was detected in CAFs, compared to NFs. Therefore, we believed MEG3 released from CAFs promotes cell viability, metastasis, and chemoresistance. In addition, growing evidence has indicated that exosomes are secreted by CAFs as the result of crosstalk between CAFs and target cancer cells³⁹ and CAFs can release exosomes to enhance tumor progression and chemoresistance.⁴⁰ In this study, we initially identified MEG3 expression in NCI-H69 and NCI-H446 cells grown in CAF-CM, which was suppressed by upon treatment with GW4869, an exosome inhibitor. These results implied that the repressed expression of MEG3 may be precisely because of inhibition of exosome secretion. Subsequently, we found that MEG3 levels were increased in CAF-derived exosomes. Importantly, research has shown that cancer cells acquire a malignant phenotype by taking up exosomes that deliver tumor-derived oncogenic factors.⁴¹ Similarly, SCLC cells co-cultured with CAF-derived exosomes showed high expression of MEG3. Therefore, we deemed that CAFs may release exosomes containing MEG3 to affect the progression and che-

moresistance of SCLC. Interestingly, a series of records has revealed that lncRNAs from CAF-derived exosomes are involved in cancer progression and immune evasion, including colorectal cancer-associated lncRNA in colorectal cancer,⁷ LINC00355 in bladder cancer,⁹ and POU3F3 in esophageal squamous cell carcinoma.¹⁰ Expounding on our findings and previous results, we suggest that MEG3 released from CAF-derived exosomes may be a crucial regulator of SCLC tumorigenesis and chemoresistance.

In summary, our present findings, for the first time, indicate that MEG3 released from exosomes derived from CAFs confers DDP resistance via regulation of a miR-15a-5p/CCNE1 axis in SCLC. This current study may provide a new potential therapeutic strategy for improving the clinical benefits of DDP chemotherapy in SCLC patients.

AUTHOR CONTRIBUTIONS

Conceptualization: Yulu Sun and Guijun Hao. **Data curation:** Yulu Sun and Guijun Hao. **Formal analysis:** Yulu Sun, Guijun Hao, Mengqi Zhuang, and Huijuan Lv. **Investigation:** Yulu Sun and Guijun Hao. **Methodology:** Chunhong Liu and Keli Su. **Project administration:** Yulu Sun and Guijun Hao. **Resources:** Yulu Sun and Guijun Hao. **Software:** Keli Su. **Supervision:** Yulu Sun and Guijun Hao. **Validation:** Chunhong Liu and Keli Su. **Visualization:** Keli Su. **Writing—original draft:** Mengqi Zhuang, Huijuan Lv, Chunhong Liu, and Keli Su. **Writing—review & editing:** Yulu Sun and Guijun Hao. **Approval of final manuscript:** all authors.

ORCID iDs

Yulu Sun <https://orcid.org/0000-0002-9625-5782>
 Guijun Hao <https://orcid.org/0000-0003-1446-5952>
 Mengqi Zhuang <https://orcid.org/0000-0001-5457-9386>
 Huijuan Lv <https://orcid.org/0000-0001-8742-4348>
 Chunhong Liu <https://orcid.org/0000-0003-0568-001X>
 Keli Su <https://orcid.org/0000-0003-4910-978X>

REFERENCES

- Shepshelovich D, Xu W, Lu L, Fares A, Yang P, Christiani D, et al. Body mass index (BMI), BMI change, and overall survival in patients with SCLC and NSCLC: a pooled analysis of the International Lung Cancer Consortium. *J Thorac Oncol* 2019;14:1594-607.
- Temraz S, Charafeddine M, Mukherji D, Shamseddine A. Trends in lung cancer incidence in Lebanon by gender and histological type over the period 2005-2008. *J Epidemiol Glob Health* 2017; 7:161-7.
- Sabari JK, Lok BH, Laird JH, Poirier JT, Rudin CM. Unravelling the biology of SCLC: implications for therapy. *Nat Rev Clin Oncol* 2017;14:549-61.
- Herrmann MK, Bloch E, Overbeck T, Koerber W, Wolff HA, Hille A, et al. Mediastinal radiotherapy after multidrug chemotherapy and prophylactic cranial irradiation in patients with SCLC--treatment results after long-term follow-up and literature overview. *Cancer Radiother* 2011; 15:81-8.
- Santaniello A, Napolitano F, Servetto A, De Placido P, Silvestris N, Bianco C, et al. Tumour microenvironment and immune evasion in EGFR addicted NSCLC: hurdles and possibilities. *Cancers (Basel)* 2019;11:1419.
- Mashouri L, Yousefi H, Aref AR, Ahadi AM, Molaei F, Alahari SK. Exosomes: composition, biogenesis, and mechanisms in cancer metastasis and drug resistance. *Mol Cancer* 2019;18:75.
- Deng X, Ruan H, Zhang X, Xu X, Zhu Y, Peng H, et al. Long non-coding RNA CCAL transferred from fibroblasts by exosomes promotes chemoresistance of colorectal cancer cells. *Int J Cancer* 2020;146:1700-16.
- Ren J, Ding L, Zhang D, Shi G, Xu Q, Shen S, et al. Carcinoma-associated fibroblasts promote the stemness and chemoresistance of colorectal cancer by transferring exosomal lncRNA H19. *Theranostics* 2018;8:3932-48.
- Yan L, Wang P, Fang W, Liang C. Cancer-associated fibroblasts-derived exosomes-mediated transfer of LINC00355 regulates bladder cancer cell proliferation and invasion. *Cell Biochem Funct* 2020; 38:257-65.
- Tong Y, Yang L, Yu C, Zhu W, Zhou X, Xiong Y, et al. Tumor-secreted exosomal lncRNA POU3F3 promotes cisplatin resistance in ESCC by inducing fibroblast differentiation into CAFs. *Mol Ther Oncolytics* 2020;18:1-13.
- Zhang J, Liu SC, Luo XH, Tao GX, Guan M, Yuan H, et al. Exosomal long noncoding RNAs are differentially expressed in the cervicovaginal lavage samples of cervical cancer patients. *J Clin Lab Anal* 2016;30:1116-21.
- Narayanan D, Mandal R, Hardin H, Chanana V, Schwalbe M, Rosenbaum J, et al. Long non-coding RNAs in pulmonary neuroendocrine neoplasms. *Endocr Pathol* 2020;31:254-63.
- Wu RR, Zhong Q, Liu HF, Liu SB. Role of miR-579-3p in the development of squamous cell lung carcinoma and the regulatory mechanisms. *Eur Rev Med Pharmacol Sci* 2019;23:9464-70.
- Zeng F, Wang Q, Wang S, Liang S, Huang W, Guo Y, et al. Linc00173 promotes chemoresistance and progression of small cell lung cancer by sponging miR-218 to regulate Etk expression. *Oncogene* 2020; 39:293-307.
- Ye M, Wei T, Wang Q, Sun Y, Tang R, Guo L, et al. TSPAN12 promotes chemoresistance and proliferation of SCLC under the regulation of miR-495. *Biochem Biophys Res Commun* 2017;486: 349-56.
- Chava S, Reynolds CP, Pathania AS, Gorantla S, Poluektova LY, Coulter DW, et al. miR-15a-5p, miR-15b-5p, and miR-16-5p inhibit tumor progression by directly targeting MYCN in neuroblastoma. *Mol Oncol* 2020;14:180-96.
- Wang ZM, Wan XH, Sang GY, Zhao JD, Zhu QY, Wang DM. miR-15a-5p suppresses endometrial cancer cell growth via Wnt/ β -catenin signaling pathway by inhibiting WNT3A. *Eur Rev Med Pharmacol Sci* 2017;21:4810-8.
- Yuan JH, Li WX, Hu C, Zhang B. Upregulation of SNHG12 accelerates cell proliferation, migration, invasion and restrain cell apoptosis in breast cancer by enhancing regulating SALL4 expression via sponging miR-15a-5p. *Neoplasma* 2020;67:861-70.
- Ni Y, Yang Y, Ran J, Zhang L, Yao M, Liu Z, et al. miR-15a-5p inhibits metastasis and lipid metabolism by suppressing histone acetylation in lung cancer. *Free Radic Biol Med* 2020;161:150-62.
- Ergun S, Güney S, Temiz E, Petrovic N, Gunes S. Significance of miR-15a-5p and CNKSR3 as novel prognostic biomarkers in non-small cell lung cancer. *Anticancer Agents Med Chem* 2018;18: 1695-701.
- Gorski JW, Ueland FR, Kolesar JM. CCNE1 amplification as a predictive biomarker of chemotherapy resistance in epithelial ovarian cancer. *Diagnostics (Basel)* 2020;10:279.
- Yang R, Xing L, Zheng X, Sun Y, Wang X, Chen J. The circRNA circAGFG1 acts as a sponge of miR-195-5p to promote triple-nega-

- tive breast cancer progression through regulating CCNE1 expression. *Mol Cancer* 2019;18:4.
23. Zhu W, Si Y, Xu J, Lin Y, Wang JZ, Cao M, et al. Methyltransferase like 3 promotes colorectal cancer proliferation by stabilizing CCNE1 mRNA in an m6A-dependent manner. *J Cell Mol Med* 2020;24:3521-33.
 24. Liang Y, Zhang D, Li L, Xin T, Zhao Y, Ma R, et al. Exosomal microRNA-144 from bone marrow-derived mesenchymal stem cells inhibits the progression of non-small cell lung cancer by targeting CCNE1 and CCNE2. *Stem Cell Res Ther* 2020;11:87.
 25. Walter RF, Werner R, Ting S, Vollbrecht C, Theegarten D, Christoph DC, et al. Identification of deregulation of apoptosis and cell cycle in neuroendocrine tumors of the lung via NanoString nCounter expression analysis. *Oncotarget* 2015;6:24690-8.
 26. Pu D, Hou M, Li Z, Zeng X. [A randomized controlled study of chemotherapy: etoposide combined with oxaliplatin or cisplatin regimens in the treatment of extensive-stage small cell lung cancer in elderly patients]. *Zhongguo Fei Ai Za Zhi* 2013;16:20-4.
 27. Rossman J, Reddy V, Cantor A, Miley D, Robert F. Phase II study of dose-intense chemotherapy with sequential topoisomerase-targeting regimens with irinotecan/oxaliplatin followed by etoposide/carboplatin in chemotherapy naive patients with extensive small cell lung cancer. *Lung Cancer* 2011;72:219-23.
 28. Zhang Y, Li Y, Han L, Zhang P, Sun S. SBF2-AS1: an oncogenic lncRNA in small-cell lung cancer. *J Cell Biochem* 2019;120:15422-8.
 29. Niu Y, Ma F, Huang W, Fang S, Li M, Wei T, et al. Long non-coding RNA TUG1 is involved in cell growth and chemoresistance of small cell lung cancer by regulating LIMK2b via EZH2. *Mol Cancer* 2017;16:5.
 30. Sun Y, Hu B, Wang Q, Ye M, Qiu Q, Zhou Y, et al. Long non-coding RNA HOTTIP promotes BCL-2 expression and induces chemoresistance in small cell lung cancer by sponging miR-216a. *Cell Death Dis* 2018;9:85.
 31. Deng R, Fan FY, Yi H, Liu F, He GC, Sun HP, et al. MEG3 affects the progression and chemoresistance of T-cell lymphoblastic lymphoma by suppressing epithelial-mesenchymal transition via the PI3K/mTOR pathway. *J Cell Biochem* 2019;120:8144-53.
 32. Li H, Wang P, Liu J, Liu W, Wu X, Ding J, et al. Hypermethylation of lncRNA MEG3 impairs chemosensitivity of breast cancer cells. *J Clin Lab Anal* 2020;34:e23369.
 33. Li L, Shang J, Zhang Y, Liu S, Peng Y, Zhou Z, et al. MEG3 is a prognostic factor for CRC and promotes chemosensitivity by enhancing oxaliplatin-induced cell apoptosis. *Oncol Rep* 2017;38:1383-92.
 34. Gao Q, Fang X, Chen Y, Li Z, Wang M. Exosomal lncRNA UCA1 from cancer-associated fibroblasts enhances chemoresistance in vulvar squamous cell carcinoma cells. *J Obstet Gynaecol Res* 2021;47:73-87.
 35. Wang D, Wu W, Huang W, Wang J, Luo L, Tang D. LncRNA LUADT1 sponges miR-15a-3p to upregulate Twist1 in small cell lung cancer. *BMC Pulm Med* 2019;19:246.
 36. Tommelein J, Verset L, Boterberg T, Demetter P, Bracke M, De Wever O. Cancer-associated fibroblasts connect metastasis-promoting communication in colorectal cancer. *Front Oncol* 2015;5:63.
 37. Paulsson J, Rydén L, Strell C, Frings O, Tobin NP, Fornander T, et al. High expression of stromal PDGFR β is associated with reduced benefit of tamoxifen in breast cancer. *J Pathol Clin Res* 2017;3:38-43.
 38. Cruz-Bermúdez A, Laza-Briviesca R, Vicente-Blanco RJ, García-Grande A, Coronado MJ, Laine-Menéndez S, et al. Cancer-associated fibroblasts modify lung cancer metabolism involving ROS and TGF- β signaling. *Free Radic Biol Med* 2019;130:163-73.
 39. Fatima F, Nawaz M. Stem cell-derived exosomes: roles in stromal remodeling, tumor progression, and cancer immunotherapy. *Chin J Cancer* 2015;34:541-53.
 40. Fan Q, Yang L, Zhang X, Peng X, Wei S, Su D, et al. The emerging role of exosome-derived non-coding RNAs in cancer biology. *Cancer Lett* 2018;414:107-15.
 41. Becker A, Thakur BK, Weiss JM, Kim HS, Peinado H, Lyden D. Extracellular vesicles in cancer: cell-to-cell mediators of metastasis. *Cancer Cell* 2016;30:836-48.